# Improved Exact Evaluation of Equal-Gain Diversity Receivers in Rayleigh Fading Channels

**FERNANDO ALMEIDA GARCÍA**[ID][1], **(Member, IEEE), HENRY CARVAJAL MORA**[ID][2], **(Senior Member, IEEE), AND NATHALY OROZCO GARZÓN**[ID][2], **(Member, IEEE)**

[1] School of Electrical and Computer Engineering, University of Campinas (UNICAMP), Campinas 13083-852, Brazil
[2] Faculty of Engineering and Applied Sciences (FICA), Telecommunications Engineering, Universidad de Las Américas (UDLA), Quito 170125, Ecuador

Corresponding author: Henry Carvajal Mora (henry.carvajal@udla.edu.ec)

**ABSTRACT** In this paper, we evaluate the performance of equal-gain-combining (EGC) receivers operating in Rayleigh fading channels in terms of the outage probability (OP) and the average symbol error rate (ASER). For this, we first derive novel, improved, fast, and exact series representations for the probability density function (PDF) and the cumulative distribution function (CDF) of the sum of independent and identically distributed Rayleigh random variables by employing complex analysis as well as the properties of the moment-generating function (MGF). With these results, exact and closed-form-asymptotic expressions to evaluate the OP and the ASER are derived. The efficiency of our expressions, defined in terms of tractability, computational burden, and computation time, overcome the state-of-the-art solutions. Monte-Carlo simulations and a time comparison analysis with the state-of-the-art study support our results.

**INDEX TERMS** Equal-gain-combining, Rayleigh-fading, outage-probability, average symbol error rate.

## I. INTRODUCTION

One of the fifth-generation (5G) mobile systems use cases is associated with ultra-reliable-low-latency communications (URLLC) [1], [2], that among some technical aspects, imply a very high reliability, or equivalently, a very low outage probability (OP) [3]. To guarantee the values set for these key-performance indicators (KPIs), future wireless systems are expected to employ different techniques, among which we can highlight spatial diversity obtained with a large number of receiving antennas [4].

In wireless systems, the received signals are randomly attenuated. This attenuation is modeled as a channel gain that multiplies the signal, and its envelope is known as fading [5]. It is well-known in the literature that an antenna array at the receiver combats the undesirable fading effects since spatial diversity is obtained. However, to exploit this diversity, it is also necessary to use combination techniques. In single-user scenarios without the presence of interference, the best performing combination technique is maximal ratio combining (MRC), which requires perfect knowledge of

the fading amplitude for proper operation [6], [7]. This makes its practical implementation difficult, mainly when the number of diversity branches is high. More specifically, MRC requires a phase compensation stage, which can be implemented through a phase-locked loop (PLL) circuit and, additionally, requires knowledge of the fading amplitude since the received signals at each diversity branch must be multiplied by the fading amplitude, thus affecting that branch [6]. Then, the resulting signals are coherently summed. The knowledge of the fading amplitude at the receiver involves the use of pilot symbols and channel estimation techniques [8]. MRC has been widely studied in the literature and exact closed-form expressions are available in the literature to analyze different performance parameters [6]. On the other hand, a sub-optimal single-user combination technique that does not require knowledge of the instantaneous fading amplitude is equal-gain-combining (EGC), where only a coherent sum of the signals obtained via spatial diversity, thus, only a phase compensation stage is required by this receiver [7]. Consequently, the practical implementation of EGC becomes simpler than that of MRC.

The performance analysis of EGC diversity receivers involves the sum of fading random variables (RVs) [9], [10].

The associate editor coordinating the review of this manuscript and approving it for publication was Faissal El Bouanani[ID].

In particular, when there is non-line-of-sight (NLOS) between the transmitter and the receiver, the fading can be modeled by a Rayleigh distribution [11], [12]. Nevertheless, the statistical analysis of the sum of Rayleigh RVs is intricate due to the cumbersome mathematics involved. This has motivated the development of improved and approximate expressions.

Some approximations and upper bounds have been proposed for the sum of Rayleigh RVs. Upper bounds for the cumulative distribution function (CDF) of a weighted sum of independent and identically distributed (i.i.d.) Rayleigh RVs were presented in [13], [14]. Moreover, in [15], the author derived a highly accurate, closed-form approximation for the CDF of the sum of i.i.d. Rayleigh variates based on the small argument approximation (SAA) technique. In [16] and [17], accurate approximations for the probability density function (PDF) of the sum of i.i.d. Nakagami-$m$ and $\alpha$–$\mu$ RVs were respectively derived via estimators based on moments. Nakagami-$m$ and $\alpha$–$\mu$ distributions are of importance here as they comprise the Rayleigh distribution. Specifically, the Rayleigh PDF is obtained from the Nakagami-$m$ and $\alpha$–$\mu$ distributions by employing the following parameter setup: $m = 1$, $\alpha = 2$, and $\mu = 1$ [16], [18].

Other works are based on exact solutions. An exact PDF for the sum of two independent Rayleigh RVs is obtained in [19]. In [20], an infinite series representation for the PDF and CDF was derived at the cost of convergence problems, and a high number of terms is required in the series for a large number of Rayleigh RVs. Moreover, in [21], the authors presented a nested series representation for the sum PDF of i.i.d. Nakagami-$m$ RVs. These expressions become computational intractable when the number of Nakagami-$m$ RVs exceeds six. In [22], a closed-form PDF solution was derived for the sum of independent, but not necessarily identically distributed (i.n.i.d.) Nakagami-$m$ RVs. The PDF is presented in terms of the Lauricella multivariable hypergeometric function [23], which is not implemented as a routine in software. In addition, as its definition relies on nested infinite sums [23, Appendix (A.20)], its computational implementation can be costly and prone to convergence/instability problems as the number of RVs in the sum increases. In [24], a sum of correlated and i.n.i.d. Nakagami-$m$ random variables is considered, where approximations are used to model the statistical distributions of the sum and the results are applied for the performance analysis of EGC receivers. In scenarios related to reconfigurable and large intelligent surfaces, the sum of random variables also appears. More specifically, the distribution of the sum of the product of random variables is required for their performance analysis. This scenario goes beyond the analysis presented in this work, but the reader may refer to [25], [26], where approximate expressions have been found for the PDF of the considered sum.

By the above, some works in the literature have evaluated the performance of EGC by obtaining approximate expressions to evaluate various KPIs in different operation scenarios. For example, in [27], the author obtains upper-bounds for the OP and the average symbol error probability (ASEP) and lower-bounds for the Shannon average spectral efficiency of EGC systems operating in Nakagami-$m$ fading channels. Numerical results show that the obtained upper-bounds are not accurate if $m = 1$, that is, in a Rayleigh fading channel. Moreover, as the number of branches increases, the difference between simulated and theoretical results also increases. Approximate infinite series expressions to evaluate the ASEP are also derived in [28]. In particular, this work focuses on developing a new approximation method for the computation of the required coefficients of the error probability series. In [29], by considering the sum of Nakagami-$m$ RVs, a closed-form PDF approximation was proposed, which is valid for identical and integer $m$ parameters. The derived PDF is valid for correlated Nakagami-$m$ RVs, and the approximation is used to evaluate the performance of EGC receivers. The results show that the proposed PDF ensures a good approximation as the parameter $m$ increases. A similar work considering correlated Nakagami-$m$ fading envelopes is presented in [30], where expressions to evaluate the ASEP are presented. Although the expressions proposed in this work require a low computational burden, they are not in full agreement with the results obtained through simulation.

Few works have obtained exact expressions for evaluating KPIs for EGC systems. For instance, exact non-closed-form expressions for the ASEP of an EGC system, which selects the 2 largest branches out of $N$ available, were derived in [31]. In [32], the authors presented an expression for the PDF of the signal-to-noise ratio (SNR) at the output of dual-diversity EGC receivers over Rayleigh fading. With this result, closed-form expressions for the ASEP of M-ary phase-shift keying (M-PSK) signals were obtained. Finally, exact average capacity expressions for EGC in correlated and uncorrelated general fading channels were obtained in [33] via a moment-generating function (MGF)-based approach. The obtained expressions are expressed in integral form, in which the integration kernel is composed of sums-products of Fox's H functions [23]. Unfortunately, the Fox's H function is not implemented as a routine in software, turning its implementation a bit fiddly. More recently, in [34], the author derived exact series representations for the average bit error rate (ABER) of a 4-branch EGC receiver subject to independent Rayleigh fading. To do so, the author relied on the simplification of the product of two Gauss hypergeometric functions. Unfortunately, no PDF nor CDF expressions for the sum of independent Rayleigh RVs were provided. As can be seen, the search for exact solutions for the KPIs of EGC receivers under Rayleigh is still an open problem in the literature, in which only costly or limited solutions (up to 4 branches) exist so far.

In this work, we perform an improved exact closed-form evaluation of EGC receivers in Rayleigh fading channels. For this, we first derive improved expressions for the PDF and CDF of the sum of i.i.d. Rayleigh RVs, which provide more tractable and less time-consuming solutions than those in [22, eq. (4)], that is the state-of-the-art study regarding the sum of independent Nakagami-$m$ and Rayleigh RVs. It is important to highlight that, unlike previous works, the

mathematical complexity of the PDF and CDF does not increase as the number of RVs grows. With these results at hand, exact and closed-form-asymptotic expressions are derived to evaluate the OP and the ASER of EGC systems. These expressions can be easily evaluated by employing common computing software.

The remainder of this paper is organized as follows. The novel PDF and CDF expressions for the sum of i.i.d. Rayleigh RVs are derived in Section II. The performance evaluation of EGC receivers is carried out in Section III and is given in terms of the OP and the ASER. Some numerical results and relevant discussions are carried out in Section IV. Finally, the main conclusions are detailed in Section V.

## II. PDF AND CDF DERIVATION OF THE SUM OF i.i.d. RAYLEIGH RVs

Since fading is a multiplicative factor to the transmitted signal and because EGC adds the received signals, a sum of random fading amplitudes is performed at the receiver. In this section, novel PDF and CDF expressions for the sum of i.i.d. Rayleigh RVs are obtained.

Let $Z$ be the sum of $N$ i.i.d. Rayleigh RVs $X_n$, that is,

$$Z = \sum_{n=1}^{N} X_n, \tag{1}$$

where the PDF and CDF of each random variable $X_n$ are respectively given by [11]

$$f_{X_n}(x_n) = \frac{x_n}{\sigma^2} \exp\left(-\frac{x_n^2}{2\sigma^2}\right), \quad x_n \geq 0 \tag{2}$$

$$F_{X_n}(x_n) = 1 - \exp\left(-\frac{x_n^2}{2\sigma^2}\right), \quad x_n \geq 0 \tag{3}$$

where $\sigma > 0$ is the scale parameter. In addition, for Rayleigh fading, $2\sigma^2$ is the fading mean power.

By the above, our next aim is obtaining the PDF and the CDF of $Z$, defined in (1), in an exact, more tractable, and less time-consuming form. This analysis is carried out in the next subsections.

### A. PDF

First, we calculate the MGF for the PDF of $X_n$, that is,

$$
\begin{aligned}
\mathcal{M}_{X_n}(s) &\triangleq \mathbb{E}\left[\exp\left(-sx_n\right)\right] \\
&= \int_0^\infty \exp(-sx_n) f_{X_n}(x_n) \mathrm{d}x_n \\
&= \underbrace{\int_0^\infty \exp\left(-sx_n\right) \frac{x_n}{\sigma^2} \exp\left(-\frac{x_n^2}{2\sigma^2}\right) \mathrm{d}x_n}_{\mathcal{I}_1}, \tag{4}
\end{aligned}
$$

where $\mathbb{E}[\cdot]$ denotes expectation and $s$ is a complex number. Notice that the integral $\mathcal{I}_1$ converges for $\forall s \in \mathbb{C}$. In fact, the integral $\mathcal{I}_1$ can be easily integrated by parts, yielding to a well-known result [5]:

$$\mathcal{M}_{X_n}(s) = 1 + \sqrt{\frac{\pi}{2}} s\sigma \exp\left(\frac{s^2\sigma^2}{2}\right) \left[\mathrm{erf}\left(\frac{s\sigma}{\sqrt{2}}\right) + 1\right], \tag{5}$$

where $\mathrm{erf}(\cdot)$ is the Gauss error function [35, eq. (7.2.2)].

Instead of using (5), we decide to manipulate (4) a little more, i.e.,

$$
\begin{aligned}
\mathcal{M}_{X_n}(s) &\overset{(a)}{=} \int_0^\infty \exp\left(-\frac{x_n^2}{2\sigma^2}\right) \frac{x_n}{\sigma^2} \left(\frac{1}{2\pi j}\right) \\
&\quad \times \oint_{\mathcal{C}_{S_1}} \Gamma(s_1)(sx_n)^{-s_1} \mathrm{d}s_1 \, \mathrm{d}x_n \\
&\overset{(b)}{=} \frac{1}{\sigma^2}\left(\frac{1}{2\pi j}\right) \oint_{\mathcal{C}_{S_1}} \Gamma(s_1)(s)^{-s_1} \\
&\quad \times \underbrace{\int_0^\infty x_n^{1-s_1} \exp\left(-\frac{x_n^2}{2\sigma^2}\right) \mathrm{d}x_n}_{\mathcal{I}_2} \mathrm{d}s_1, \tag{6}
\end{aligned}
$$

where step (a) employs the contour integral definition over the first exponential function, i.e., $\exp(-sx_n)$, [35, eq. (16.17.1)], and step (b) interchanges the order of integration as $\int_0^\infty |\exp(-sx_n) f_{X_n}(x_n)| \, \mathrm{d}x_n < \infty$. Here, $\mathcal{C}_{S_1}$ is a contour that encloses the poles of the function $\Gamma(s_1)$ in the positive sense (counterclockwise sense) [36]. Notice that the integral $\mathcal{I}_2$ converges in the region $\mathbf{Re}[s_1] < 2$, where $\mathbf{Re}[\cdot]$ denotes the real part of its argument. That is, we exchange an expression that is entire in the complex plane by another one that only converges in the region $\mathbf{Re}[s_1] < 2$.

Now, solving $\mathcal{I}_2$ and after some simplifications, we obtain

$$\mathcal{M}_{X_n}(s) = \left(\frac{1}{2\pi j}\right) \oint_{\mathcal{C}_{S_2}} \frac{\Gamma(s_1)\Gamma(1-s_1/2)}{\left(\sqrt{2}s\sigma\right)^{s_1}} \mathrm{d}s_1, \tag{7}$$

in which $\mathcal{C}_{S_2}$ is a complex contour, which is presented because the second integral deformed the integration path of $\mathcal{C}_{S_1}$. For the integral to converge, it is required that the poles of $\Gamma(s_1)$ to be distinct from those of $\Gamma(1-s_1/2)$ [23], [37]. Thus, $\mathcal{C}_{S_2}$ can be defined as a contour that encloses the poles of the function $\Gamma(1-s_1/2)$ in the negative sense (clockwise sense). Observe that (7) is now a meromorphic function analytically defined on the strip $0 < s_1 < 2$ and with singularities located at $s_1 = -\ell$ and $s_1 = 2(1+\ell)$, $\ell \in \mathbb{N}$, i.e., the natural integers.

This new contour representation allows us to break the MGF of $f_{X_n}(x_n)$ in both a convergent and a divergent part. For instance, if we take the singularities at $s_1 = -\ell$ (which is the region where $\mathcal{I}_2$ is well-defined, i.e., $\mathbf{Re}[s_1] < 2$) and then using Cauchy's residue theorem to evaluate the contour integral over $s_1$, we obtain (5), which is the standard MGF of a Rayleigh RV. On the other hand, if we consider the singularities at $2(1+\ell)$ (which is the region where $\mathcal{I}_2$ is not defined, i.e., $\mathbf{Re}[s_1] \geq 2$) and then applying Cauchy's residue theorem, we obtain

$$\mathcal{M}_{X_n}(s) = \frac{1}{s^2\sigma^2} \sum_{\ell=0}^\infty \frac{1}{\ell!} \Gamma[2(\ell+1)]\left(-2\sigma^2 s^2\right)^{-\ell}, \tag{8}$$

which is a divergent series.

For independent RVs, the PDF of the sum of these RVs is obtained as the convolution of the marginal PDFs, that is,

$$f_Z(z) = f_{X_1}(x_1) * f_{X_2}(x_2) * \cdots * f_{X_N}(x_N). \tag{9}$$

It is well-known that the MGF of the convolution of $N$ functions is equal to the product of the MGFs of each function [38]. By employing this property in (9), we obtain

$$\mathcal{M}_Z(s) = \prod_{n=1}^{N} \mathcal{M}_{X_n}(s) \tag{10}$$
$$\stackrel{(a)}{=} [\mathcal{M}_{X_n}(s)]^N.$$

where step (a) considers that all the RVs are identically distributed.

To obtain the PDF of $Z$, we need to perform the MGF inversion, i.e.,

$$f_Z(z) = \left(\frac{1}{2\pi j}\right) \oint_{\mathcal{C}_{S_3}} \exp(sz)\, \mathcal{M}_Z(s)\, \mathrm{d}s$$

$$\stackrel{(a)}{=} \left(\frac{1}{2\pi j}\right) \oint_{\mathcal{C}_{S_3}} \exp(sz)$$

$$\times \left[\left(\frac{1}{2\pi j}\right) \oint_{\mathcal{C}_{S_2}} \frac{\Gamma(s_1)\,\Gamma(1-s_1/2)}{\left(\sqrt{2}s\sigma\right)^{s_1}} \mathrm{d}s_1\right]^N \mathrm{d}s, \tag{11}$$

in which $\mathcal{C}_{S_3}$ is the Bromwich contour [39] and step (a) employs (7) and (10).

From (5) and (8), it can be seen that (11) takes the form of the so-called divergent integrals since it is composed of a convergent and divergent part, depending on the region that we choose for $s_1$ [40]–[42]. There are different ways of interpreting these types of divergent integrals. In this work, we interpret them via analytic continuation [43]–[45]. More specifically, we employ Cauchy's residue formula to remove the divergence and to analytically continue (11) to the whole complex plane, i.e., $s_1 \in \mathbb{C}$. To proceed with this, we substitute (8) into (11), resulting in

$$f_Z(z) = \frac{1}{\sigma^{2N}} \left(\frac{1}{2\pi j}\right) \oint_{\mathcal{C}_{S_3}} \frac{\exp(sz)}{s^{2N}} \left(\sum_{\ell=0}^{\infty} s^{-2\ell} \kappa_\ell\right)^N \mathrm{d}s, \tag{12}$$

where $\kappa_\ell$ is defined as

$$\kappa_\ell = \frac{\Gamma[2(\ell+1)]\left(-2\sigma^2\right)^{-\ell}}{\ell!}. \tag{13}$$

Next, similar to [46, eq. (2.7)], we utilize the following equality:

$$\left(\sum_{\ell=0}^{\infty} s^{-2\ell} \kappa_\ell\right)^N = \sum_{\ell=0}^{\infty} s^{-2\ell} \zeta_\ell. \tag{14}$$

Now, after differentiating both sides of (14) with respect to $s^{-2}$, it follows that the coefficients $\zeta_\ell$ can be obtained recursively by

$$\zeta_\ell = \begin{cases} 1, & \ell = 0 \\ \dfrac{1}{\ell} \displaystyle\sum_{p=1}^{\ell} \dfrac{1}{p!}(p-\ell+Np) \dfrac{\Gamma[2(p+1)]}{\left(-2\sigma^2\right)^p} \zeta_{\ell-p}, & \ell \geq 1. \end{cases} \tag{15}$$

After substituting (15) into (14) and then, the resulting expression into (12), we get

$$f_Z(z) = \frac{1}{\sigma^{2N}} \left(\frac{1}{2\pi j}\right) \oint_{\mathcal{C}_{S_3}} \frac{\exp(sz)}{s^{2N}} \sum_{\ell=0}^{\infty} s^{-2\ell} \zeta_\ell\, \mathrm{d}s. \tag{16}$$

Notice that we have purposely introduced a singularity of order $2(N+\ell)$ at $s = 0$. This will allow us to evaluate the above integral by using Cauchy's residue formula. More importantly, since $2(N+\ell) \in \{2, 4, 6, 8, \ldots\}$ is always a positive integer greater than or equal to 2, then no cut branches are needed in the Bromwich contour to make the integrand of (16) a single-valued function. If on the other hand, we substitute (5) into the MGF inversion formula, we will not be able to apply the sum of residues since the resulting expression will not generate poles.[1] This is because (5) is well-defined $\forall s \in \mathbb{C}$.

Finally, after the integration of each term and employing Cauchy's residue theorem [38, Appendix A], (16) reduces to

$$f_Z(z) = \frac{1}{\sigma^{2N}} \sum_{\ell=0}^{\infty} \frac{z^{2(\ell+N)-1}}{\Gamma[2(\ell+N)]} \zeta_\ell. \tag{17}$$

Appendix A shows that (17) converges absolutely. As a simple verification example, for $N = 1$, (17) reduces to the PDF of a single Rayleigh RV, meaning that the MGF inversion analytically continues (16) $\forall s \in \mathbb{C}$ (see Appendix B). Moreover, if $\mathfrak{T}_0$ terms are employed in the PDF defined by (17), its truncation error can be written as

$$\mathfrak{T}_{f_Z} = \frac{1}{\sigma^{2N}} \sum_{\ell=\mathfrak{T}_0}^{\infty} \frac{z^{2(N+\ell)-1}}{\Gamma[2(N+\ell)]} \zeta_\ell, \tag{18}$$

which can be bounded by (19), located at the bottom of the next page, (for better understanding of this result see Appendix C). In (19), ${}_3\tilde{F}_3(a_1, a_2, a_3; b_1, b_2, b_3; c) = {}_3F_3(a_1, a_2, a_3; b_1, b_2, b_3; c) / \Gamma(b_1)\Gamma(b_2)\Gamma(b_3)$ is the regularized generalized hypergeometric function [47, eq. (1.2.23)].

It is important to highlight that (17) enjoys a lower computation burden than [21, eq. (10)] and [22, eq. (4)] in which an additional summation is needed for each new Rayleigh RV in the sum. On the contrary, the mathematical complexity of (17) does not increase with $N$. This can be easily confirmed by inspection.

### B. CDF

The CDF of $Z$ can be easily obtained from (17) by employing [11]

$$F_Z(z) = \int_0^z f_Z(u)\, \mathrm{d}u$$

$$= \frac{1}{\sigma^{2N}} \int_0^z \sum_{\ell=0}^{\infty} \frac{u^{2(\ell+N)-1}}{\Gamma[2(\ell+N)]} \zeta_\ell\, \mathrm{d}u. \tag{20}$$

---

[1]It is worth mentioning that other approaches can be used to solve (16) without using Cauchy's residue theorem, for instance, by explicitly evaluating the integral over the contour $\mathcal{C}_{S_3}$ by a proper parameterization. Of course, this approach will be more mathematically involved.

Since (17) converges absolutely, we can interchange the integration order of (20) [48]. Thus, doing this interchange and then evaluating the resulting integral, we obtain

$$F_Z(z) = \frac{1}{\sigma^{2N}} \sum_{\ell=0}^{\infty} \frac{z^{2(\ell+N)}}{\Gamma[2(\ell+N)+1]} \zeta_\ell. \tag{21}$$

The proof of the absolute convergence of (21) is presented in Appendix D. Additionally, if $\mathfrak{T}_0$ terms are considered in the CDF defined by (21), we can write its truncation error as

$$\mathfrak{T}_{F_Z} = \frac{1}{\sigma^{2N}} \sum_{\ell=\mathfrak{T}_0}^{\infty} \frac{z^{2(N+\ell)}}{\Gamma[2(N+\ell)+1]} \zeta_\ell, \tag{22}$$

which can be bounded by (23), located at the top of this page, and that is derived in Appendix E.

The tractability of (17) and (21) paves the way for the analytical derivation of performance metrics of several wireless communication systems that involve the sum of Rayleigh RVs, that, in most cases, are hampered by complex mathematics. As an application of this, we analyze the performance of EGC receivers in the next section. Moreover, one can rely on (19) and (23), as shown at the bottom of the page, to efficiently determine how many terms are needed in the sum PDF and CDF to guarantee the desired accuracy.

## III. PERFORMANCE EVALUATION OF EGC RECEIVERS

In this section, we evaluate the performance of an $N$-branch EGC system affected by Rayleigh fading in terms of the OP and the ASER. More specifically, exact and closed-form-asymptotic expressions for these performance indicators are obtained.

In an $N$-branch EGC diversity receiver where the additive white noise has the same power level at each branch, the instantaneous SNR at the output of the combiner can be written as [5]

$$\Psi = \frac{1}{N} \gamma_0 \left( \sum_{n=1}^{N} X_n \right)^2$$
$$= \frac{1}{N} \gamma_0 Z^2, \tag{24}$$

where $\{X_n\}_{n=1}^{N}$ are the i.i.d. Rayleigh envelopes and $\gamma_0 = E_s/N_0$, where $E_s$ is the average received energy per symbol on a unit-gain link, and $N_0$ denotes the unilateral noise power spectral density, thus, $\gamma_0$ is the received SNR per symbol. Before proceeding to the performance analysis of this EGC receiver, it is convenient to derive the PDF and the CDF of its output SNR.

From (17), the PDF of $\Psi$ can be easily calculated through a transformation of variables, i.e,

$$f_\Psi(\psi) = \frac{N}{2\sigma^{2N}} \frac{1}{\gamma_0} \sum_{\ell=0}^{\infty} \frac{\left(\frac{1}{\gamma_0}N\psi\right)^{\ell+N-1}}{\Gamma[2(\ell+N)]} \zeta_\ell. \tag{25}$$

Notice that (25) converges absolutely as it was obtained using a direct variable transformation of (17).

From (25), the CDF of $\Psi$ can be obtained as

$$F_\Psi(\psi) = \int_0^\psi f_\Psi(u)\mathrm{d}u$$
$$= \frac{N}{2\sigma^{2N}} \frac{1}{\gamma_0} \int_0^\psi \sum_{\ell=0}^{\infty} \frac{\left(\frac{1}{\gamma_0}Nu\right)^{\ell+N-1}}{\Gamma[2(\ell+N)]} \zeta_\ell \, \mathrm{d}u. \tag{26}$$

Then, we interchange the integration order and evaluate the remaining integral, leading up to

$$F_\Psi(\psi) = \frac{N}{2\sigma^{2N}} \frac{1}{\gamma_0} \sum_{\ell=0}^{\infty} \frac{\left(\frac{1}{\gamma_0}N\right)^{\ell+N-1} \psi^{\ell+N}}{(\ell+N)\Gamma[2(\ell+N)]} \zeta_\ell. \tag{27}$$

The integration order in (26) can be performed due to the absolute convergence of (25).

Finally, making use of $1/a\Gamma(2a) = 2/\Gamma(2a+1)$ along with some minor simplifications, we obtain

$$F_\Psi(\psi) = \frac{1}{\sigma^{2N}} \sum_{\ell=0}^{\infty} \frac{\left(\frac{1}{\gamma_0}N\psi\right)^{\ell+N}}{\Gamma(2\ell+2N+1)} \zeta_\ell. \tag{28}$$

Following the same approach as in Appendix D, it can be shown that (28) also converges absolutely.

In the literature, the OP is usually defined in terms of the instantaneous SNR [5, eq. (9.184)] or in terms of the instantaneous capacity [49, eq. (4)]. Thus, expressions to calculate the OP of EGC receivers considering both definitions are obtained below.

### A. OP FROM THE INSTANTANEOUS SNR
Considering the instantaneous SNR, $\Psi$, the OP is defined as the probability that $\Psi$ falls below a certain threshold $\gamma_{th}$, that is [5],

$$P_{\Psi,\mathrm{out}} = \Pr[\Psi \leq \gamma_{th}]$$
$$= \int_0^{\gamma_{th}} f_\Psi(\psi)\mathrm{d}\psi. \tag{29}$$

Therefore, the OP can be obtained from (28) evaluated at $\gamma_{th}$, i.e.,

$$P_{\Psi,\mathrm{out}} = F_\Psi(\gamma_{th})$$
$$= \frac{1}{\sigma^{2N}} \sum_{\ell=0}^{\infty} \frac{\left(\frac{1}{\gamma_0}N\gamma_{th}\right)^{\ell+N}}{\Gamma(2\ell+2N+1)} \zeta_\ell. \tag{30}$$

$$\mathfrak{T}_{f_Z} < \frac{\sqrt{\pi} N \Gamma(2\mathfrak{T}_0+2) z^{2N+2\mathfrak{T}_0-1} \, {}_3\tilde{F}_3\left(1, \mathfrak{T}_0+1, \mathfrak{T}_0+\frac{3}{2}; \mathfrak{T}_0, N+\mathfrak{T}_0, N+\mathfrak{T}_0+\frac{1}{2}; \frac{z^2}{2\sigma^2}\right)}{2^{2N+3\mathfrak{T}_0-1}\sigma^{2(N+\mathfrak{T}_0)}}. \tag{19}$$

$$\mathfrak{T}_{F_Z} < \frac{\sqrt{\pi} N \Gamma(2\mathfrak{T}_0+2) \left(\frac{z}{\sigma}\right)^{2(N+\mathfrak{T}_0)} \, {}_3\tilde{F}_3\left(1, \mathfrak{T}_0+1, \mathfrak{T}_0+\frac{3}{2}; \mathfrak{T}_0, N+\mathfrak{T}_0+\frac{1}{2}, N+\mathfrak{T}_0+1; \frac{z^2}{2\sigma^2}\right)}{2^{2N+3\mathfrak{T}_0}}. \tag{23}$$

In the high SNR regime, i.e., when $\gamma_0 \rightarrow \infty$, the most significant term in the summation of (30) occurs for $\ell = 0$. Thus, considering only this term, the asymptotic OP can be obtained as

$$P_{\Psi,\text{out}} \simeq \frac{\left(\frac{1}{\gamma_0} N \gamma_{\text{th}}\right)^N}{\sigma^{2N} \Gamma(2N+1)}. \tag{31}$$

### B. OP FROM THE INSTANTANEOUS CAPACITY

On the other hand, if the instantaneous system capacity, $C(\Psi)$, is considered, the OP can be expressed as [49]

$$P_{C,\text{out}} = \Pr\left[C(\Psi) < r_{\text{th}}\right], \tag{32}$$

where $r_{\text{th}}$ is a threshold rate and the capacity for a wireless transmission can be obtained as [5]

$$C(\Psi) = W \log_2(1 + \Psi), \tag{33}$$

where $W$ denotes the employed bandwidth, and $\Psi$ is the SNR, given by (24). Therefore, employing (28), (32) can be rewritten as

$$P_{C,\text{out}} = F_\Psi\left(2^{r_{\text{th}}/W} - 1\right)$$
$$= \frac{1}{\sigma^{2N}} \sum_{\ell=0}^{\infty} \frac{\left[\frac{1}{\gamma_0} N \left(2^{r_{\text{th}}/W} - 1\right)\right]^{\ell+N}}{\Gamma(2\ell + 2N + 1)} \zeta_\ell. \tag{34}$$

The asymptotic OP can be obtained by using the first term of the summation in (34), yielding to

$$P_{C,\text{out}} \simeq \frac{1}{\sigma^{2N}\Gamma(2N+1)} \left[\frac{1}{\gamma_0} N \left(2^{\frac{r_{\text{th}}}{W}} - 1\right)\right]^N. \tag{35}$$

From (31) and (35), notice that the OP is proportional to $\gamma_0^{-N}$. Thus, $N$ represents the system diversity order. This result corroborates our mathematical modeling.

### C. ASER

Another KPI often used to EGC receivers is the ASER, defined as [5, eq. (9.61)]

$$P_e = \int_0^\infty Q\left(\sqrt{2\mathcal{P}\psi}\right) f_\Psi(\psi)\mathrm{d}\psi, \tag{36}$$

where $\mathcal{P}$ is a modulation dependent constant and $Q(\cdot)$ is the Gaussian Q-function [5, eq. (4.2)].

Replacing (25) into (36) and followed by some algebraic manipulations with the aid of [35, eq. (7.1)], yields to

$$P_e = \frac{1}{2\sigma^{2N}} \sum_{\ell=0}^{\infty} \frac{\left(\frac{N}{4\gamma_0\mathcal{P}}\right)^{\ell+N}}{\Gamma(\ell+N+1)} \zeta_\ell. \tag{37}$$

The asymptotic ASER at a high SNR can be obtained by considering the first term of the series in (37), resulting in

$$P_e \simeq \frac{\left(\frac{N}{4\gamma_0\mathcal{P}\sigma^2}\right)^N}{2\Gamma(N+1)}. \tag{38}$$

Notice that all derived performance metrics expressions, exact and asymptotic, can be quickly executed using well-known mathematical functions that are available in common mathematical packages.
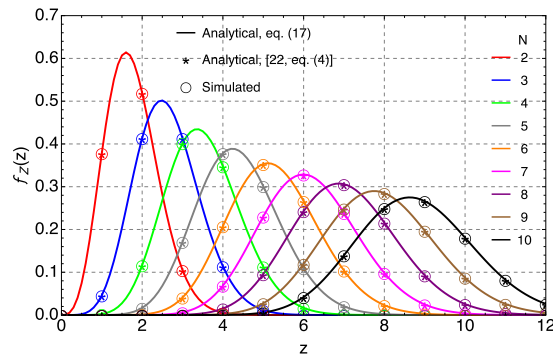
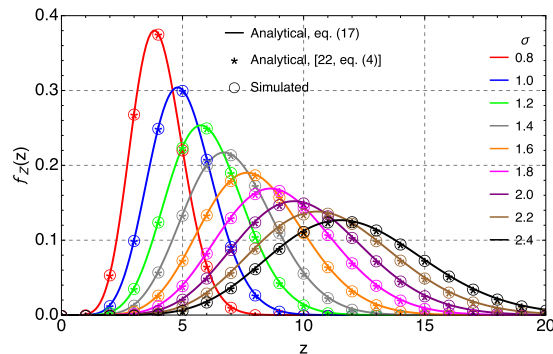**FIGURE 1.** PDF of $Z$ considering $\sigma = 7/10$ and different values of $N$.



**FIGURE 2.** PDF of $Z$ considering $N = 4$ and different values of $\sigma$.

## IV. NUMERICAL RESULTS AND DISCUSSIONS

In this section, the performance of EGC receivers is assessed employing our derived expressions in some scenarios. Moreover, we assess the efficiency of (17), expressed in terms of computational burden and computation time, compared to the state-of-the-art solution given by [22, eq. (4)]. The efficiency of (21) is not presented herein since there are no new exact competing studies regarding the sum CDF. Monte-Carlo simulations validate our analysis.[2] For the analysis, we employed the mathematical software Wolfram Mathematica running over a 1.4 GHz Quad-Core Intel i5 processor.

At this point, it is important to indicate that the values of the simulation parameters used in this section are arbitrary values that allow observing the wide range of operation of the theoretical expressions derived in previous sections.

Figs. 1 and 2 show simulated and theoretical PDFs of $Z$, given by (17), for different values of $N$ and $\sigma$. On the other hand, Figs. 3 and 4 show simulated and analytical CDFs of $Z$, given by (21), for different values of $N$ and $\sigma$. In addition, the analytical results of [22, eq. (4)] are also considered in these figures for comparison purposes. In the results, notice the perfect agreement between our expressions, the result of [22, eq. (4)], and the simulations.

To evaluate the efficiency of (17), we take as an example 10 test scenarios which are presented in Table 1. In this table, $f_Z^\dagger(z)$ denotes the PDF of $Z$ obtained by numerically

---

[2]The number of Monte-Carlo trials was set to $10^7$.

**TABLE 1.** Test scenarios and absolute errors.

| Scenario | Parameter settings | $f_Z^\dagger(z)$ | $\epsilon^{(1)}$ | $\epsilon^{(2)}$ |
|---|---|---|---|---|
| 1 | $\sigma = 0.7, N = 4, z = 3$ | 0.4017 | $4.9133 \times 10^{-10}$ | $5.4221 \times 10^{-10}$ |
| 2 | $\sigma = 1.5, N = 4, z = 7$ | 0.2017 | $5.4693 \times 10^{-10}$ | $9.4345 \times 10^{-10}$ |
| 3 | $\sigma = 0.9, N = 5, z = 7$ | 0.1631 | $1.4572 \times 10^{-10}$ | $2.1493 \times 10^{-10}$ |
| 4 | $\sigma = 1.1, N = 5, z = 7$ | 0.2421 | $8.3566 \times 10^{-10}$ | $8.0232 \times 10^{-10}$ |
| 5 | $\sigma = 0.6, N = 6, z = 5$ | 0.3421 | $9.2576 \times 10^{-10}$ | $7.2411 \times 10^{-10}$ |
| 6 | $\sigma = 0.8, N = 6, z = 5$ | 0.2472 | $2.4563 \times 10^{-10}$ | $4.2145 \times 10^{-10}$ |
| 7 | $\sigma = 1.2, N = 7, z = 10$ | 0.1900 | $9.4632 \times 10^{-10}$ | $4.5113 \times 10^{-10}$ |
| 8 | $\sigma = 1.4, N = 7, z = 10$ | 0.1150 | $4.3531 \times 10^{-10}$ | $5.3511 \times 10^{-10}$ |
| 9 | $\sigma = 1.5, N = 8, z = 13$ | 0.1174 | $1.3341 \times 10^{-10}$ | $8.9532 \times 10^{-10}$ |
| 10 | $\sigma = 1.6, N = 8, z = 13$ | 0.0862 | $2.6899 \times 10^{-10}$ | $5.2513 \times 10^{-10}$ |

**TABLE 2.** Efficiency comparison of (17) and [22, eq. (4)].

| Scenario | Terms for (17) | Computation Time for (17) [$s$] | Computation Time for [22, eq. (4)] [$s$] | Time Saving [%] |
|---|---|---|---|---|
| 1 | 25 | 0.0060 | 0.1845 | 96.74 |
| 2 | 25 | 0.0046 | 0.1507 | 96.91 |
| 3 | 75 | 0.0562 | 3.0072 | 98.13 |
| 4 | 75 | 0.0566 | 3.9592 | 98.57 |
| 5 | 80 | 0.0647 | 8.8656 | 99.27 |
| 6 | 80 | 0.0585 | 6.8923 | 99.15 |
| 7 | 82 | 0.0730 | 10.897 | 99.33 |
| 8 | 82 | 0.0749 | 13.622 | 99.45 |
| 9 | 85 | 0.0532 | 15.657 | 99.66 |
| 10 | 85 | 0.0678 | 16.165 | 99.58 |



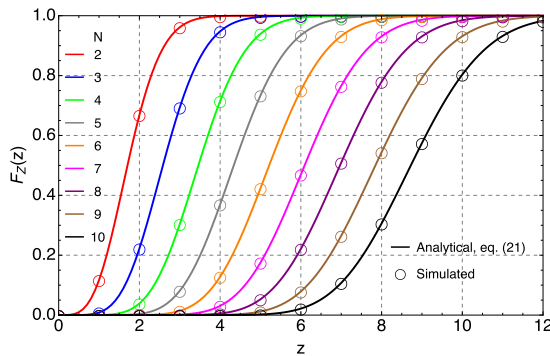**FIGURE 3.** CDF of *Z* considering $\sigma = 7/10$ and different values of *N*.



**FIGURE 4.** CDF of *Z* considering $N = 4$ and different values of $\sigma$.

evaluating the multi-fold Brennan's integral [19],[3] and $\epsilon^{(1)}$ and $\epsilon^{(2)}$ respectively denote the absolute errors for (17) and [22, eq. (4)], computed by

$$\epsilon^{(\ell)} = \left| f_Z^\dagger(z) - f_Z^{(\ell)}(z) \right|, \qquad (39)$$

for $\ell = 1, 2$. Thus, $f_Z^{(1)}(z)$ and $f_Z^{(2)}(z)$ are the PDFs of *Z* calculated via (17) and [22, eq. (4)], respectively.

From the setup defined in Table 1, in Table 2 we show the efficiency of our mathematical modeling through the number of terms required for evaluating (17), as well as the computation time for evaluating this expression and [22, eq. (4)], and the time saving when our derived PDF expression is employed. The number of terms required and the computation time were obtained when (17) and [22, eq. (4)] achieve an absolute target error, say, around $10^{-10}$, as observed in Table 1. Thus, it is interesting to observe in

---

[3]Herein, we used the numerical integration method "GlobalAdaptive" of the MATHEMATICA software employing an accuracy goal of $10^{-10}$.
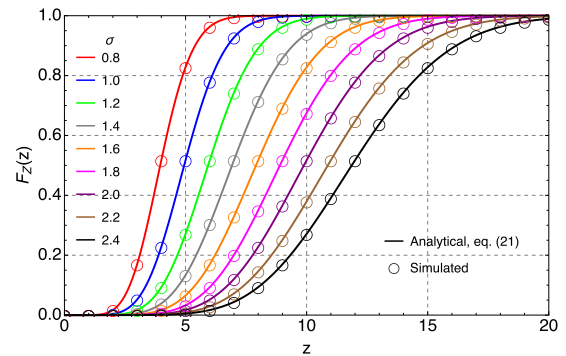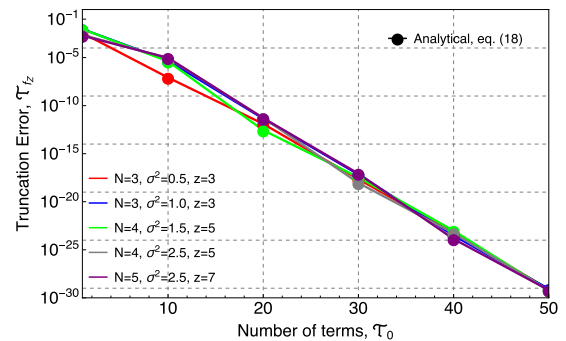


**FIGURE 5.** Truncation error, $\mathfrak{T}_{f_Z}$, considering and different values of *N*, $\sigma$, and *z*.

the second column of Table 2 that no more than 85 terms were needed in any scenario. In addition, the computation time is greatly reduced, showing impressive reductions of above 96% in the considered scenarios.

Figs. 5 and 6 depict the truncation errors, eqs. (18) and (22), as a function of the number of terms $\mathfrak{T}_0$. Notice how
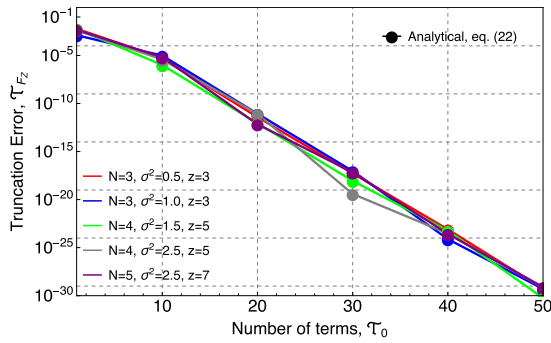
**FIGURE 6.** Truncation error, $\mathfrak{T}_{F_Z}$, considering and different values of $N$, $\sigma$, and $z$.
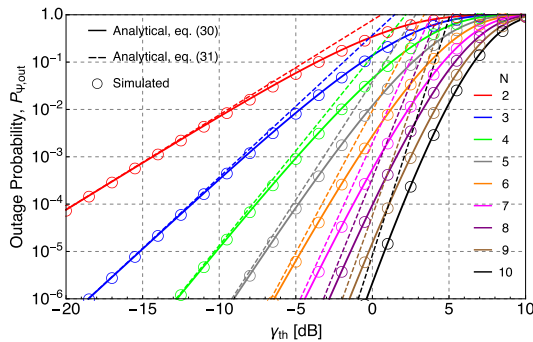


**FIGURE 7.** $P_{\Psi,out}$ versus $\gamma_{th}$ considering $\sigma = 1$, $\gamma_0 = 0.46$, and different values of $N$.
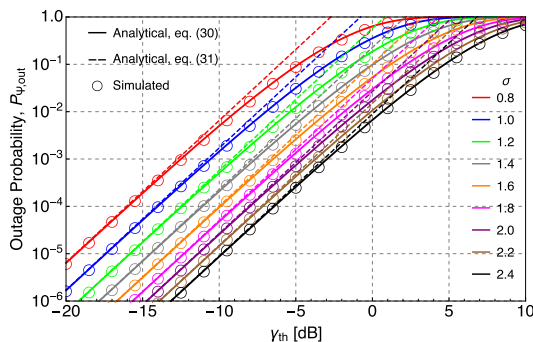


**FIGURE 8.** $P_{\Psi,out}$ versus $\gamma_{th}$ considering $N = 3$, $\gamma_0 = 0.28$, and different values of $\sigma$.



**FIGURE 9.** $P_{C,out}$ versus $r_{th}/W$ using $\sigma = 0.7$ and different values of $N$.
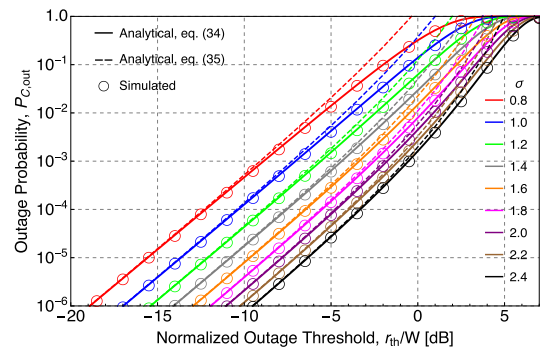


**FIGURE 10.** $P_{C,out}$ versus $r_{th}/W$ using $N = 3$ and different values of $\sigma$.



**FIGURE 11.** $P_e$ versus $\gamma_0$ considering $N = 2$, $\mathcal{P} = 1$, and different values of $\sigma$.

the truncation errors decrease as we increase the number of terms. Notably, no more than 20 terms are required in (18) and (22) to ensure an error less than $10^{-10}$, which is an acceptable error for some practical scenarios.

Figs. 7 and 8 show analytical and simulated OPs obtained from the instantaneous SNR considering different values of $N$ and $\sigma$, respectively. The analytical results are obtained using 100 terms in (30). Notice that given a certain threshold $\gamma_{th}$, the OPs decrease as $\sigma$ or $N$ increase, which is an expected result. Specifically, when $\sigma$ increases, the fading mean power increases, consequently, the received SNR increases, and the system has a better performance. Moreover, when $N$ increases, the number of diversity branches increases, and the EGC receiver can better combat the undesirable fading channel effects. In addition, for a given $N$ or $\sigma$, as $\gamma_{th}$
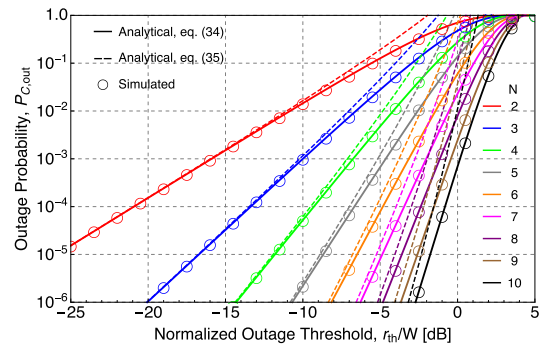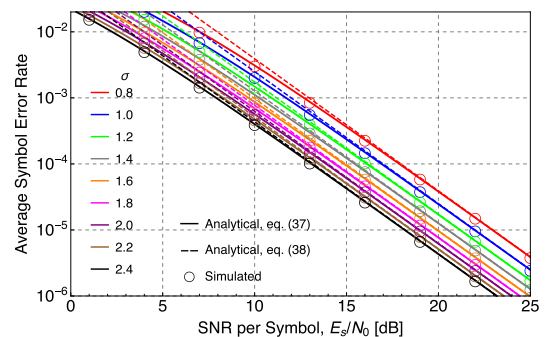
increases, the OP also increases because a higher minimum SNR is established for a proper system operation.

Figs. 9 and 10 show the analytical and simulated OPs obtained from the instantaneous capacity considering different values of $N$ and $\sigma$, respectively. The analytical results are obtained employing 100 terms in (34). In Figs. 9 and 10, the OP curves show a similar behavior to those of Figs. 7 and 8, respectively. That is, given a threshold rate, the OP decreases as $\sigma$ or $N$ grows. Equivalently, for a given $N$ or $\sigma$, as $r_{th}/W$ increases, the OP increases as well. At this point, it is important to highlight that, unlike previous works, the mathematical complexity of all our derived expressions does not increase as the number of RVs in the sum grows, or equivalently, the number of diversity branches grows. This can be easily verified by a close inspection of (17), (21), (30) and (34).
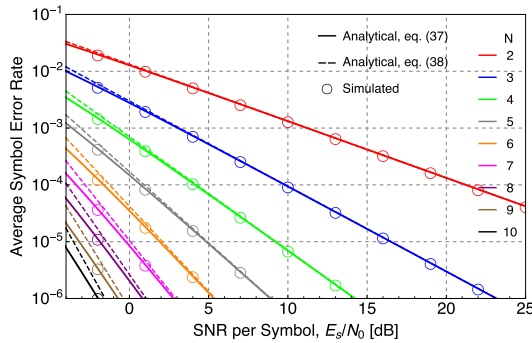
**FIGURE 12.** $P_e$ versus $\gamma_0$ considering $\sigma = 3.4$, $\mathcal{P} = 1$, and different values of $N$.

Fig. 11 depicts the exact and asymptotic ASER versus $\gamma_0$ considering $N = 2$, $\mathcal{P} = 1$, and various values of $\sigma$. Moreover, Fig. 12 illustrates the exact and asymptotic ASER as a function of $\gamma_0$, considering $\sigma = 3.4$, $\mathcal{P} = 1$, and various values of $N$. Observe how our exact curves perfectly coincide with the numerical simulations. In addition, notice how the ASERs decrease as either $\gamma_0$, $\sigma$ or $N$ increases. In the latter case, the system diversity is increased. This can be also noticed in the asymptote given by (38).

## V. CONCLUSION

In this paper, we derived novel exact expressions for the PDF and CDF of the sum of i.i.d. Rayleigh variates, which are interesting analytical tools as they allow for noticeable savings in computational load and execution time compared to state-of-the-art studies. To achieve this, we employed a comprehensive complex analysis and modeling based on the manipulation of infinite series.

With our novel expressions, we evaluated, in exact and asymptotic manner, the performance of an $N$-branch EGC system over Rayleigh fading channels. Exact and closed-form-asymptotic expressions were obtained for the OP and the ASER. The PDF and CDF expressions derived in this work can be employed in other areas or applications where the sum of Rayleigh random variables appear, such as signal detection, intersymbol interference, and interference estimation [50]–[53]. In addition, the mathematical modeling presented in this work can also be employed in other scenarios where the sum of i.i.d. random variables appear as long as the MGF of the sum exits.

.

## APPENDIX A
### ABSOLUTE CONVERGENCE OF THE SUM PDF
If (17) converges absolutely, then the following must be fulfilled [54]:

$$\sum_{\ell=0}^{\infty} \frac{|\zeta_\ell| \, z^{2(N+\ell)-1}}{\Gamma[2(N+\ell)]} < \infty. \tag{40}$$

From (15), the absolute value of $\zeta_\ell$, for $\ell \geq 1$, can be bounded as

$$|\zeta_\ell| < \frac{1}{\ell} \sum_{p=1}^{\ell} \frac{|Np+p-\ell| \, |\zeta_{\ell-p}| \, \Gamma[2(p+1)] \, (2\sigma^2)^{-p}}{p!}. \tag{41}$$

Thus, after taking the absolutes values in (41) and using the fact that $N\ell \geq |Np + p - \ell|$ for $1 \leq p \leq \ell$, one attains

$$|\zeta_\ell| < N \sum_{p=1}^{\ell} \frac{|\zeta_{\ell-p}| \, \Gamma[2(p+1)] \, (2\sigma^2)^{-p}}{p!}. \tag{42}$$

Notice that (42) is a positive increasing function that grows with $\ell$. Hence, after using the last term of the sum ($p = \ell$) and then multiplying the resulting expression by $\ell$, we obtain

$$|\zeta_\ell| < \frac{N\Gamma[2(\ell+1)] \, (2\sigma^2)^{-\ell}}{\Gamma(\ell)}. \tag{43}$$

Now, separating the first term of the sum in (40), we get

$$\sum_{\ell=0}^{\infty} \frac{|\zeta_\ell| \, z^{2(N+\ell)-1}}{\Gamma[2(N+\ell)]} = z^{2N-1} \left( \frac{1}{\Gamma(2N)} + \sum_{\ell=1}^{\infty} \frac{z^{2\ell} \, |\zeta_\ell|}{\Gamma[2(N+\ell)]} \right). \tag{44}$$

Finally, employing the bound (43) in (44) along with some algebraic manipulations with the aid of [47, eq. (1.2.23)], we obtain (45), as shown at the top of the next page, where $_2F_2(a_1, a_2; b_1, b_2; c)$ is the generalized hypergeometric function [47, eq. (1.2.23)]. Consequently, since the upper bound for (40) exists and is finite, it immediately follows that (17) converges absolutely.

## APPENDIX B
### SINGLE RAYLEIGH DISTRIBUTION
Considering $N = 1$, (17) reduces to

$$f_Z(z) = \frac{1}{\sigma^2} \sum_{\ell=0}^{\infty} \frac{z^{2\ell+1}}{\Gamma[2(\ell+1)]} \zeta_\ell, \tag{46}$$

and the coefficients are now given by

$$\zeta_\ell = \begin{cases} 1, & \ell = 0 \\ \dfrac{3}{2} \left( -\dfrac{2}{\sigma^2} \right)^\ell \left( \dfrac{5}{2} \right)_{\ell-1}, & \ell \geq 1 \end{cases} \tag{47}$$

where $(\cdot)_{(\cdot)}$ represents the pochhammer symbol [35, eq. (5.2.3)].

Replacing (47) into (46) and separating the first term of the summation, we obtain

$$f_Z(z) = \frac{z}{\sigma^2} \left[ 1 + \frac{3}{2} \sum_{\ell=1}^{\infty} \frac{\left( -\frac{2z^2}{\sigma^2} \right)^\ell}{\Gamma[2(\ell+1)]} \left( \frac{5}{2} \right)_{\ell-1} \right]. \tag{48}$$

Finally, after applying [55, eq. (5.2.11.1)] and some algebraic manipulations, we obtain the PDF of a single Rayleigh RV, i.e.,

$$f_Z(z) = \frac{z}{\sigma^2} \exp\left( -\frac{z^2}{2\sigma^2} \right). \tag{49}$$

$$\sum_{\ell=0}^{\infty} \frac{|\zeta_\ell| \, z^{2(N+\ell)-1}}{\Gamma(2(N+\ell))} < z^{2N-1} \left[ \frac{1}{\Gamma(2N)} + \frac{3Nz^2 \, _2F_2\left(2, \frac{5}{2}; N+1, N+\frac{3}{2}; \frac{z^2}{2\sigma^2}\right)}{\sigma^2 \Gamma(2(N+1))} \right] \tag{45}$$

$$\sum_{\ell=0}^{\infty} \frac{|\zeta_\ell| \, z^{2(N+\ell)}}{\Gamma(2(N+\ell)+1)} < z^{2N} \left[ \frac{1}{\Gamma(2N+1)} + \frac{3Nz^2 \, _2F_2\left(2, \frac{5}{2}; N+\frac{3}{2}, N+2; \frac{z^2}{2\sigma^2}\right)}{\sigma^2 \Gamma(2N+3)} \right] \tag{53}$$

## APPENDIX C
### TRUNCATION ERROR FOR THE SUM PDF

An upper bound for $\mathfrak{T}_{f_Z}$, defined by (18), can be found by using the absolute value of $\zeta_i$, i.e.,

$$\mathfrak{T}_{f_Z} < \frac{z^{2N-1}}{\sigma^{2N}} \sum_{\ell=\mathfrak{T}_0}^{\infty} \frac{z^{2\ell} |\zeta_\ell|}{\Gamma[2(N+\ell)]}. \tag{50}$$

Finally, employing the bound (43) in (50) and after some simplifications by the aid of [47, eq. (1.2.23)], we obtain (19), which completes the derivation.

## APPENDIX D
### ABSOLUTE CONVERGENCE OF THE SUM CDF

If (21) converges absolutely, then the following must be fulfilled [54]:

$$\sum_{\ell=0}^{\infty} \frac{|\zeta_\ell| \, z^{2(N+\ell)}}{\Gamma[2(N+\ell)+1]} < \infty. \tag{51}$$

Separating the first term of the sum in (40), it yields

$$\sum_{\ell=0}^{\infty} \frac{|\zeta_\ell| \, z^{2(N+\ell)}}{\Gamma[2(N+\ell)+1]} = z^{2N} \left( \frac{1}{\Gamma(2N+1)} \right. $$
$$\left. + \sum_{\ell=1}^{\infty} \frac{z^{2\ell} |\zeta_\ell|}{\Gamma[2(N+\ell)+1]} \right). \tag{52}$$

Finally, employing the bound (43) in (52) and after performing some algebraic manipulations with the aid of [47, eq. (1.2.23)], we obtain (53), as shown at the top of this page. Therefore, as the upper bound for (51) exists and it is finite, it immediately follows that (21) converges absolutely.

## APPENDIX E
### TRUNCATION ERROR FOR THE SUM CDF

An upper bound for $\mathfrak{T}_{F_Z}$, defined by (22), can be obtained using the absolute value of $\zeta_i$, thus,

$$\mathfrak{T}_{F_Z} < \left(\frac{z}{\sigma}\right)^{2N} \sum_{\ell=\mathfrak{T}_0}^{\infty} \frac{z^{2\ell} |\zeta_\ell|}{\Gamma(2(N+\ell)+1)}. \tag{54}$$

After employing the bound (43) in (54) along with some simplifications by the aid of [47, eq. (1.2.23)], we obtain the result of (23).

## REFERENCES

[1] A. Ghosh, A. Maeder, M. Baker, and D. Chandramouli, "5G evolution: A view on 5G cellular technology beyond 3GPP release 15," *IEEE Access*, vol. 7, pp. 127639–127651, 2019.

[2] P. Browna, S. E. Elayoubi, M. Deghel, and A. Galindo-Serrano, "Design and performance evaluation of contention-based transmission schemes for URLLC services," *Perform. Eval.*, vol. 143, pp. 1–14, Nov. 2020.

[3] A. Traßl, E. Schmitt, T. Hößler, L. Scheuvens, N. Franchi, N. Schwarzenberg, and G. Fettweis, "Outage prediction for ultra-reliable low-latency communications in fast fading channels," *EURASIP J. Wireless Commun. Netw.*, vol. 2021, no. 1, pp. 1–25, Dec. 2021.

[4] E. A. Jorswieck and H. Boche, "Outage probability in multiple antenna systems," *Eur. Trans. Telecommun.*, vol. 18, no. 3, pp. 217–233, 2007.

[5] M. K. Simon and M.-S. Alouini, *Digital Communication Over Fading Channels*, 2nd ed. Hoboken, NJ, USA: Wiley, 2005.

[6] J. G. Proakis, *Digital Communications*, 3rd ed. New York, NY, USA: McGraw-Hill, 1995.

[7] J. R. Barry, E. A. Lee, and D. G. Messerschmitt, *Digital Communication*, 3rd ed. New York, NY, USA: Springer, 2003.

[8] C. D. Altamirano, J. Minango, H. C. Mora, and C. De Almeida, "BER evaluation of linear detectors in massive MIMO systems under imperfect channel estimation effects," *IEEE Access*, vol. 7, pp. 174482–174494, 2019.

[9] Y. Song, S. D. Blostein, and J. Cheng, "Exact outage probability for equal gain combining with cochannel interference in Rayleigh fading," *IEEE Trans. Wireless Commun.*, vol. 2, no. 5, pp. 865–870, Sep. 2003.

[10] V. Ramanathan and A. Annamalai, "Analysis of equal gain diversity receivers in correlated Rayleigh fading channels," *IEEE Commun. Lett.*, vol. 8, no. 6, pp. 362–364, Jun. 2004.

[11] A. Papoulis, *Probability, Random Variables, and Stochastic Processes*, 4th ed. New York, NY, USA: McGraw-Hill, 2002.

[12] H. I. Cho, C. Y. Lee, and G. U. Hwang, "Performance analysis of single source and single relay cooperative ARQ protocols under time correlated Rayleigh fading channel," *Perform. Eval.*, vol. 68, no. 5, pp. 395–413, May 2011.

[13] P. Hitczenko, "A note on a distribution of weighted sums of i.i.d. Rayleigh random variables," *Sankhyā, Indian J. Statist., A*, vol. 60, no. 2, pp. 171–175, 1998.

[14] G. K. Karagiannidis, T. A. Tsiftsis, and N. C. Sagias, "A closed-form upper-bound for the distribution of the weighted sum of Rayleigh variates," *IEEE Commun. Lett.*, vol. 9, no. 7, pp. 589–591, Jul. 2005.

[15] J. Hu and N. C. Beaulieu, "Accurate simple closed-form approximations to Rayleigh sum distributions and densities," *IEEE Commun. Lett.*, vol. 9, no. 2, pp. 109–111, Feb. 2005.

[16] D. B. da Costa, M. D. Yacoub, and J. C. S. S. Filho, "An improved closed-form approximation to the sum of arbitrary Nakagami-*m* variates," *IEEE Trans. Veh. Technol.*, vol. 57, no. 6, pp. 3854–3858, Nov. 2008.

[17] D. B. da Costa, M. D. Yacoub, and J. C. S. S. Filho, "Highly accurate closed-form approximations to the sum of $\alpha$–$\mu$ variates and applications," *IEEE Trans. Wireless Commun.*, vol. 7, no. 9, pp. 3301–3306, Sep. 2008.

[18] M. Nakagami, "The *m*-distribution—A general formula of intensity distribution of rapid fading," *Stat. Methods Radio Wave Propag.*, vol. 26, no. 2, pp. 3–36, Apr. 1960.

[19] D. G. Brennan, "Linear diversity combining techniques," *Proc. IRE*, vol. 47, no. 6, pp. 1075–1102, Jun. 1959.

[20] N. C. Beaulieu, "An infinite series for the computation of the complementary probability distribution function of a sum of independent random variables and its application to the sum of Rayleigh random variables," *IEEE Trans. Commun.*, vol. 38, no. 9, pp. 1463–1474, Sep. 1990.

[21] P. Dharmawansa, N. Rajatheva, and K. Ahmed, "On the distribution of the sum of Nakagami-*m* random variables," *IEEE Trans. Commun.*, vol. 55, no. 7, pp. 1407–1416, Jul. 2007.

[22] M. A. Rahman and H. Harada, "New exact closed-form PDF of the sum of Nakagami-*m* random variables with applications," *IEEE Trans. Commun.*, vol. 59, no. 2, pp. 395–401, Feb. 2011.

[23] A. M. Mathai, R. K. Saxena, and H. J. Haubold, *The H-Function: Theory and Applications*. New York, NY, USA: Springer, 2009.

[24] Z. Hadzi-Velkov, N. Zlatanov, and G. K. Karagiannidis, "An accurate approximation to the distribution of the sum of equally correlated Nakagami-*m* envelopes and its application in equal gain diversity receivers," in *Proc. IEEE Int. Conf. Commun.*, Jun. 2009, pp. 1–5.

[25] A.-A. A. Boulogeorgos and A. Alexiou, "Performance analysis of reconfigurable intelligent surface-assisted wireless systems and comparison with relaying," *IEEE Access*, vol. 8, pp. 94463–94483, 2020.

[26] F. A. P. de Figueiredo, M. S. P. Facina, R. C. Ferreira, Y. Ai, R. Ruby, Q.-V. Pham, and G. Fraidenraich, "Large intelligent surfaces with discrete set of phase-shifts communicating through double-Rayleigh fading channels," *IEEE Access*, vol. 9, pp. 20768–20787, 2021.

[27] N. C. Sagias, "Closed-form analysis of equal-gain diversity in wireless radio networks," *IEEE Trans. Veh. Technol.*, vol. 56, no. 1, pp. 173–182, Jan. 2007.

[28] H. Samimi and P. Azmi, "A simple method to approximate the probability of error for equal gain combiner over independent fading channels," *Int. J. Commun. Syst.*, vol. 21, no. 7, pp. 681–694, Jul. 2008.

[29] N. Zlatanov, Z. Hadzi-Velkov, and G. K. Karagiannidis, "An efficient approximation to the correlated Nakagami-*m* sums and its application in equal gain diversity receivers," *IEEE Trans. Wireless Commun.*, vol. 9, no. 1, pp. 302–310, Jan. 2010.

[30] M. Harada, "Asymptotic performance analysis of reception diversity with coherent detection in Nakagami-rice fading channels," *IEICE Commun. Exp.*, vol. 2, no. 2, pp. 18–24, 2013.

[31] P. Polydorou and P. Ho, "Symbol error probability for double selection/equal gain combining of branches in a Rayleigh fading environment without channel statistical information," in *Proc. IEEE Global Telecommun. Conf. (GLOBECOM)*, San Antonio, TX, USA, Nov. 2001, pp. 1–8.

[32] X. Qi, M. S. Alouini, and Y.-C. Ko, "Closed-form analysis of dual-diversity equal-gain combining over Rayleigh fading channels," *IEEE Trans. Wireless Commun.*, vol. 2, no. 6, pp. 1120–1125, Nov. 2003.

[33] F. Yilmaz and M.-S. Alouini, "A unified MGF-based capacity analysis of diversity combiners over generalized fading channels," *IEEE Trans. Commun.*, vol. 60, no. 3, pp. 862–875, Mar. 2012.

[34] Q. T. Zhang, "Error rates for 4-branch equal-gain combining in independent Rayleigh fading: A simple explicit solution," *IEEE Commun. Lett.*, vol. 26, no. 2, pp. 269–272, Feb. 2022, doi: 10.1109/LCOMM.2021.3133140.

[35] F. W. J. Olver, D. W. Lozier, R. F. Boisvert, and C. W. Clark, *NIST Handbook of Mathematical Functions*, 1st ed. Washington, DC, USA: U.S. Department of Commerce: National Institute of Standards and Technology (NIST), 2010.

[36] M. Abramowitz and I. A. Stegun, *Handbook of Mathematical Functions With Formulas, Graphs, and Mathematical Tables*, 10th ed. Washington, DC, USA: U.S. Department of Commerce: National Bureau of Standards, 1972.

[37] R. Beals and J. Szmigielski, "Meijer G-functions: A gentle introduction," *Notices Amer. Math. Soc.*, vol. 60, pp. 866–873, Aug. 2013.

[38] J. J. Distefano, A. R. Stubberud, and I. J. Williams, *Feedback Systems and Control, Schaum's Outlines*, 3rd ed. Pennsylvania Plaza, NY, USA: McGraw-Hill, 1995.

[39] J. L. Schiff, *The Laplace Transform: Theory and Applications*, 1st ed. New York, NY, USA: Springer, 1999.

[40] A. Laforgia, "A theory of divergent integrals," *Appl. Math. Lett.*, vol. 22, no. 6, pp. 834–840, Jun. 2009.

[41] B. W. Ninham, "Generalized functions and divergent integrals," *Numer. Math.*, vol. 8, pp. 444–457, Nov. 1966.

[42] E. R. Caianiello, "Generalized integration procedure for divergent integrals," *Il Nuovo Cimento A*, vol. 15, no. 2, pp. 145–161, May 1973.

[43] G. Leibbrandt, "Introduction to the technique of dimensional regularization," *Rev. Mod. Phys.*, vol. 47, no. 4, pp. 849–876, Oct. 1975.

[44] Z. É. Mihálka, Á. Szabados, and P. R. Surján, "Application of the Cauchy integral formula as a tool of analytic continuation for the resummation of divergent perturbation series," *J. Chem. Phys.*, vol. 150, no. 3, Jan. 2019, Art. no. 031101.

[45] M. Suzuki, "Analytic continuation of divergent integrals with respect to a parameter—The case of perturbations to strong interactions," *Phys. Rev.*, vol. 173, no. 5, pp. 1473–1480, Sep. 1968.

[46] P. G. Moschopoulos, "The distribution of the sum of independent gamma random variables," *Ann. Inst. Statist. Math.*, vol. 37, no. 1, pp. 541–544, Dec. 1985.

[47] H. M. Srivastava and P. W. Karlsson, *Multiple Gaussian Hypergeometric Series*. New York, NY, USA: Ellis Horwood Limited, 1985.

[48] H. S. Carslaw, "Term-by-term integration of infinite series," *Math. Gazette*, vol. 13, no. 191, pp. 437–441, Dec. 1927.

[49] A. A. Farid and S. Hranilovic, "Outage capacity optimization for free-space optical links with pointing errors," *J. Lightw. Technol.*, vol. 25, no. 7, pp. 1702–1710, Jul. 2007.

[50] F. D. A. Garcia, M. A. M. Miranda, and J. C. S. S. Filho, "New findings on GLRT radar detection of non-fluctuating targets via phased arrays," *IEEE Access*, vol. 9, pp. 95622–95635, 2021.

[51] M.-S. Alouini and M. K. Simon, "Performance analysis of coherent equal gain combining over Nakagami-*m* fading channels," *IEEE Trans. Veh. Technol.*, vol. 50, no. 6, pp. 1449–1463, Nov. 2001.

[52] F. D. A. García, A. C. F. Rodriguez, G. Fraidenraich, and J. C. S. SantosFilho, "CA-CFAR detection performance in homogeneous Weibull clutter," *IEEE Geosci. Remote Sens. Lett.*, vol. 16, no. 6, pp. 887–891, Jun. 2019.

[53] S. M. Kay, *Fundamentals of Statistical Signal Processing: Estimation Theory*, 1st ed. Upper Saddle River, NJ, USA: Prentice-Hall, 1993.

[54] E. Kreyszig, *Advanced Engineering Mathematics*, 10th ed. Hoboken, NJ, USA: Wiley, 2010.

[55] A. P. Prudnikov, Y. A. Bryčkov, and O. I. Maričev, *Integral and Series*, vol. 2, 3rd ed. Moscow, Russia: Fizmatlit, 1992.

**FERNANDO ALMEIDA GARCÍA** (Member, IEEE) received the B.Sc. degree in electronics and telecommunications engineering from Armed Forces University—ESPE, Quito, Ecuador, in 2012, and the M.Sc. and Ph.D. degrees in electrical engineering from the School of Electrical and Computer Engineering (FEEC), University of Campinas (UNICAMP), São Paulo, Brazil, in 2015 and 2021, respectively. From 2014 to 2020, he worked together with Bradar Indústria S.A., a branch of Embraer Defense and Security, in the development of innovative radar processing techniques. Since 2021, he has been a Postdoctoral Fellow with the Wireless Technology Laboratory (WissTek), FEEC-UNICAMP. His research interests include radar systems, wireless communications, channel modeling, and digital signal processing.

**HENRY CARVAJAL MORA** (Senior Member, IEEE) received the B.Sc. degree (Hons.) in electronics and telecommunications engineering from Armed Forces University—ESPE, Ecuador, in 2009, and the M.Sc. and Ph.D. degrees in electrical engineering from the School of Electrical and Computer Engineering (FEEC), University of Campinas (UNICAMP), Brazil, in 2014 and 2018, respectively. He was the Director of the Technology Transfer Area in the Education, Science and Technology Secretariat (SENESCYT), Ecuador, in 2018. He obtained the HCIA-5G Certification from Huawei, in 2020. He is currently an Assistant Professor with the Universidad de Las Américas (UDLA), Ecuador. His research interests include fading channels, diversity-combining systems, orthogonal and non-orthogonal multiple access, multiuser detection, MIMO, physical-layer-security, 5G, and B5G technologies.

**NATHALY OROZCO GARZÓN** (Member, IEEE) received the Electronic and Telecommunications Engineering degree from Armed Forces University—ESPE, Ecuador, in 2011, and the M.Sc. and Ph.D. degrees in electrical engineering from the University of Campinas (UNICAMP), Brazil, in 2014 and 2018, respectively. She obtained the HCIA-5G Certification from Huawei, in 2020. She is currently an Assistant Professor with the Universidad de Las Américas (UDLA), Quito, Ecuador. Her research interests include digital communications with specific emphasis on orthogonal and non-orthogonal multiple access, fading channels, MIMO, cognitive systems, opportunistic transmissions, and 5G technologies.

● ● ●